Physics-based Analytical Formulation of the Soft Error Rate in CMOS Circuits

Jean-Luc Autran, Daniela Munteanu

Physics-based Analytical Formulation of the Soft Error Rate in CMOS Circuits

Jean-Luc Autran and Daniela Munteanu

***Abstract*— The exponential dependence of the soft-error rate (SER) with critical charge in CMOS circuits, empirically proposed by Hazucha and Svensson, is derived in the framework of the diffusion-collection approach. A full analytical formulation is established, linking the SER with physical and technological parameters, notably the circuit supply voltage, carrier diffusion coefficient and ion characteristics.**

***Index Terms*— CMOS technologies, collection-diffusion, critical charge, FinFET, numerical simulation, planar transistor, radiation effects, single event effects, soft error rate (SER), SRAM.**

I. Introduction

In the domain of single event effects in CMOS circuits, one very popular and extensively used expression is the soft error rate (SER) formula, originally proposed by Hazucha and Svensson [1]. This empirical expression links the SER and the critical charge, an essential metrics that quantifies the susceptibility of circuits to radiation [2]. Hazucha and Svensson's [1] expression can be written under the well-known form

$$SER = \kappa \cdot F \cdot A_S \cdot exp\left(-\frac{Q_{crit}}{Q_S}\right) \quad (1)$$

where κ and Q_S are two fitting parameters, F is the particle flux, A_S is the sensitive drain area (collecting node) and Q_{crit} is the critical charge. Q_S is often called collection slope, it has the same dimension as Q_{crit}, κ is dimensionless.

This expression, which empirically describes very well the dependence of the SER on the critical charge, has never been fully derived from a modeling point of view based on physics equations, even if several pioneering works by Kirkpatrick [3] and Edmonds [4,5] established all necessary physical foundations years before [1]. The aim of the present work is precisely to propose a physics-based and accessible derivation of (1) using a simple formalism in the framework of the diffusion-collection approach [3-16]. The paper is organized as follows: Section II summarizes the basic principles and main equation of the diffusion-collection model. Section III presents our analytical model of the SER and introduces a new general expression from which (1) is derived. Numerical simulations are also presented for model validation using a random-walk drift-diffusion code. Finally, Section IV discusses similarities and differences between our model and (1). It also develops the dependences of the SER with the supply voltage, inventories the model inputs, discusses possible approximations for certain parameters and provides quantitative SER trends for different bulk technological nodes. A derivation of the model for 3D FinFET architectures is finally proposed as an outline to future developments.

II. Diffusion-collection model

In the so-called "diffusion-collection" model, the energy lost by a charged particle in the semiconductor material along its track is converted into electron-hole pairs that are rearranged in the form of a succession of point charges (i.e., charges deposited in a very small volume) of electrons and holes, δn and δp, respectively, with $\delta n = \delta p = \delta n_0$ (number of pairs), just after energy deposition and creation of the pairs (Fig. 1). The model then assumes that the transport of these carriers in-excess δn (m^{-3}) is governed by a pure spherical diffusion law in the 3D semiconductor domain [6]

$$\frac{\partial \delta n(r,t)}{\partial t} - \frac{\delta n(r,t)}{\tau} = D^* \nabla^2 \delta n(r,t) \quad (2)$$

where τ is the carrier lifetime and D^* is the ambipolar diffusion coefficient given by

$$D^* = 2D_n D_p / (D_n + D_p) \quad (3)$$

with D_n and D_p are the diffusion coefficients for electrons and holes respectively.

Equation (2) can be analytically solved for all points P in space.

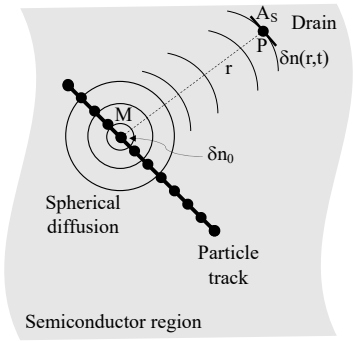

Fig. 1. Schematic illustration of the diffusion-collection model principle.

J.L. Autran, and D. Munteanu are with Aix-Marseille Université, CNRS, Université de Toulon, IM2NP (UMR 7334), F-13397 Marseille, France (e-mail: jean-luc.autran@univ-amu.fr, daniela.munteanu@univ-amu.fr).

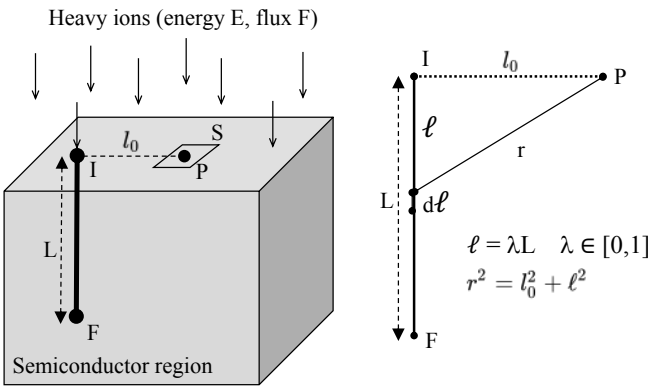

Fig. 2. Integration of (8) over an entire heavy ion track from point I to point F. The length L = IF corresponds to the particle range.

A. *Diffusion-collection considering a point source*

We first consider a unique point charge δn_0 (Dirac delta function that corresponds to a number of charges) at t=0 in M (Fig. 1). The excess carrier density (electron density in the following) at time t and distance r originating from δn_0, solution of (2), can be written under the form [6]

$$\delta n(r,t) = \frac{\delta n_0}{(4\pi D^* t)^{\frac{3}{2}}} exp\left(-\frac{r^2}{4D^* t} - \frac{t}{\tau}\right) \tag{4}$$

Considering a collecting contact (i.e., a sensitive reverse biased NMOS drain) centered in point P, the collected current at this level originating from the diffusion of the point charge δn_0 can be expressed as [7]

$$I_{col}(r,t) = qA_S v_{col} \delta n(r,t) \tag{5}$$

where A_S is, like in (1), the sensitive drain area (assumed to be small enough to avoid numerical integration in the current expression) and v_{col} is the average velocity of carriers at the level of the collection point, assimilated to the average carrier velocity in the space charge region (SCR) of the drain junction in numerous works [7-9,11-15]. Note that I_{col} must be in balance with the carrier diffusion flux (or gradient) in point P originating from δn_0 in order to maintain current continuity.

The integration over time of (5) gives the charge collected $q_{col}(r,t)$ by the contact originating from the element δn_0. Neglecting carrier recombination and putting (4) in (5), we obtain

$$q_{col}(r,t) = \frac{qA_S v_{col} \delta n_0}{4(\pi)^{\frac{3}{2}} D^* r} \times \Gamma\left(\frac{1}{2}, \frac{r^2}{4D^* t}\right) \tag{6}$$

where Γ is the upper incomplete gamma function [17]:

$$\Gamma(a,z) = \int_z^\infty t^{a-1} e^{-t} dt \tag{7}$$

For $t \to +\infty$, the gamma function term in (6) reduces to $\sqrt{\pi}$ and the collected charge at infinite time is:

$$q_{col}(r) = q\delta n_0 \times \frac{A_S v_{col}}{4\pi D^* r} \tag{8}$$

B. *Diffusion-collection considering a line source (particle track)*

From (8), it is easy to calculate the total collected charge at the drain contact resulting from the contribution of a whole particle track. For this, we consider the simplified case, shown in Fig. 2, in which a uniform beam of mono-energetic heavy ions (energy E, flux F) arrives perpendicularly to the semiconductor surface (in the following, we neglect the reflective boundary condition on the silicon surface and we consider the 3D simulation domain as an infinite medium). Assuming that the ions stop in the target material, in this case, the length of tracks L corresponds to the full range of the particles in the semiconductor. Alternatively, if the ions will not stop inside the substrate, E is replaced by the energy loss ΔE and L corresponds in this case to the thickness of the semiconductor domain crossed (see IV.A). Considering for this material an energy of electron-hole pair creation equal to $E_{e,h}$, the particle creates a total of $N = E/E_{e,h}$ (or $\Delta E/E_{e,h}$) pairs in the target material. For simplicity, we suppose a constant LET value: this charge is thus uniformly deposited along the ion track. In this case

$$\delta n_0 = \frac{N}{L} \times d\ell = \frac{E}{E_{e,h} L} \times d\ell \tag{9}$$

where ℓ and dℓ are defined in Fig. 2. Integration of (8) along the particle track in the approximation of a constant collection velocity gives

$$Q_{col} = \frac{qA_S v_{col} N}{4\pi D^*} \int_0^1 \frac{d\lambda}{\sqrt{l_0^2 + \lambda^2 L^2}} \tag{10}$$

$$\int_0^1 \frac{dx}{\sqrt{A + Bx^2}} = \frac{1}{\sqrt{B}} arsinh\left(\frac{\sqrt{B}}{\sqrt{A}}\right) \quad A, B > 0 \tag{11}$$

where *arsinh(x)* is the inverse hyperbolic sine, defined over the whole real line and given by

$$arsinh(x) = ln\left(x + \sqrt{x^2 + 1}\right) \tag{12}$$

Equation (10) finally gives

$$Q_{col} = Q_0 arsinh\left(\frac{L}{l_0}\right) \tag{13}$$

$$Q_0 = \frac{qA_S v_{col} N}{4\pi D^* L} \tag{14}$$

The form of (13) is identical to the expression (21) obtained by Edmonds in [4] for the same configuration to that of Fig. 2 but with a different boundary condition at the silicon surface (assumed to be reflective in [4]). Equation (14) is also similar but not identical to expression (24) in [4].

At this level, we can evaluate the ratio of the collected charge Q_{col} by the deposited charge $Q_{dep} = qN$. This ratio $Q_{col}/(qN)$ corresponds to a collection efficiency η_S for the collecting contact. From (13) and (14), we obtain

$$\eta_S = \frac{Q_{col}}{qN} = \frac{A_S v_{col}}{4\pi D^* L} arsinh\left(\frac{L}{l_0}\right) \qquad (15)$$

C. *Numerical verification using the RWDD approach*

To verify (8) and (15) and consequently (13) and (14), we performed extensive numerical random-walk drift-diffusion (RWDD) simulations, considering particle point sources and tracks of different lengths and distances from the collecting contact.

Fig. 3 shows the time evolution of the charge collected by a contact (0.2×0.2 µm of surface) located at 1.5 µm from the initial deposition of 40,000 electrons at t=0 (see Fig. 4). In Fig. 3, values obtained from (6) are compared to numerical simulation data obtained with a 3D Monte Carlo RWDD code [18-19]. RWDD advantageously replaces TCAD for the simplest simulations with elementary geometries and constant coefficients (field, mobility, diffusion coefficient) [20]. For memory, in the RWDD approach, each charge (or packet of charges) in excess is described as a material particle subjected to a drift-diffusion motion composed of a deterministic drift motion (in presence of an electric field **E**) and a random-walk pure diffusion. If at time t, a charge packet is located at **r**(t), after a time interval Δt, it will move to

$$\mathbf{r}(t+\Delta t) = \mathbf{r}(t) + \mu^* \Delta t \mathbf{E}(\mathbf{r}(t)) + \sqrt{2D^* \Delta t}\mathbf{N}_3(0,1) \qquad (16)$$

where $\mathbf{N}_3(0,1)$ is a 3D standard gaussian random vector and μ^* is the carrier ambipolar mobility.

In the present RWDD simulation, there is no electric field, and the numerical code simulates a pure 3D ambipolar diffusion process. The two curves of Fig. 3 are in very good agreement that illustrates the validity of (6) to describe the time dependence of the collected charge. From Fig. 3, also note the stochastics character of the RWDD curve: this is because the amount of collected charge is quite low, a few tens of electrons at the end of the transient.

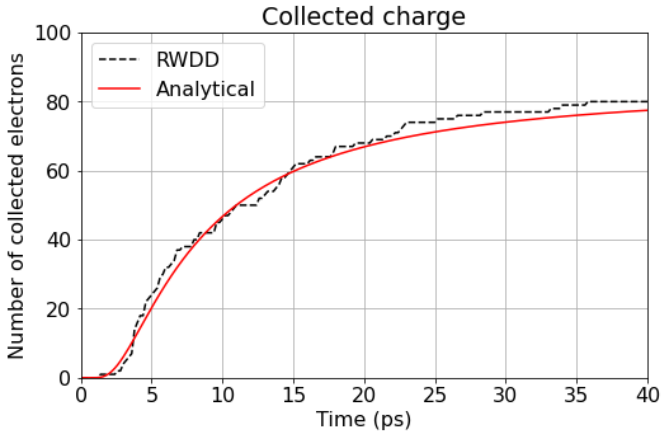

Fig. 3. Time evolution of the charge collected by a small contact (A_S = 0.2×0.2 µm²) located at a distance of 1.5 µm from the initial deposition of 40,000 electrons (see Fig. 4) analytically predicted by (6) and numerically computed using a Monte Carlo RWDD simulation code. Other values used in (6) are D^* = 533 cm²/s and v_{col} = 3.55 ×10⁶ cm/s.

In addition to Fig. 3, Fig. 4 shows four different snapshots taken at t = 0, 0.2, 2 and 20 ps after the deposition of the charges illustrating the RWDD charge transportation process. Collected carriers at the level of the contact correspond to particles reaching or passing through the surface of the contact during the simulation run.

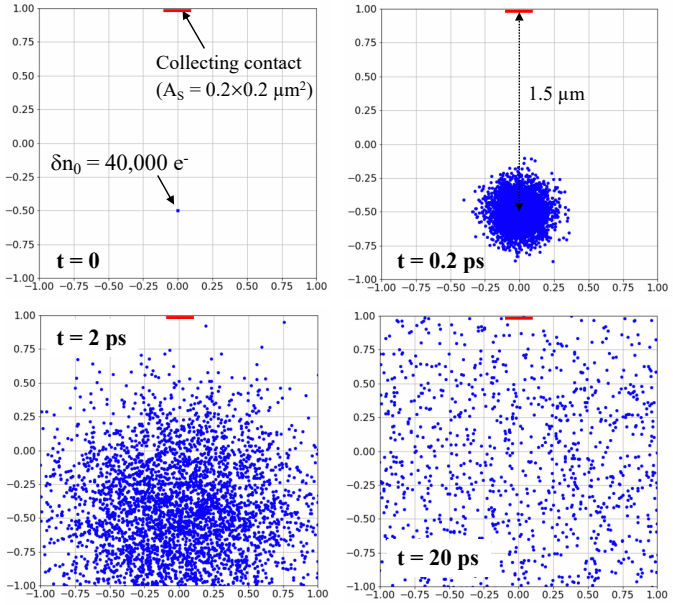

Fig. 4. Charge distributions in the projected *xz* plane (y = 0) of the 3D simulation domain at t = 0, 0.2, 2 and 20 ps after the deposition of 40,000 electrons at position (0, -0.5, 0). Charges are transported following (16) with D^* = 533 cm²/s, Δt = 0.1 ps, E = 0 (pure diffusion). The surface of the collecting contact is in the *xy* plane, perpendicular to the figure. *x* and *z* scales are in µm.

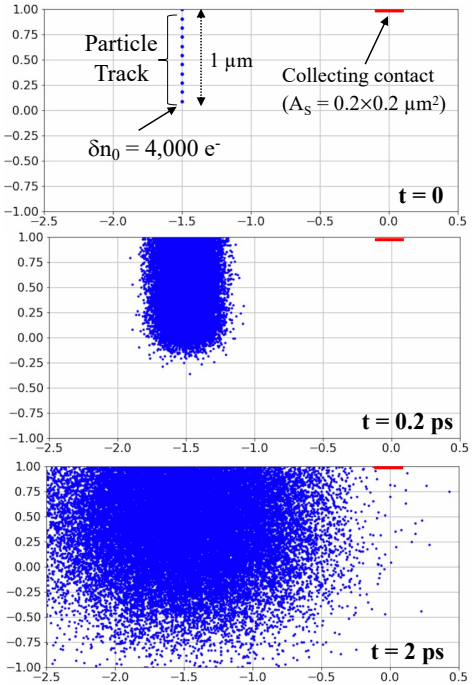

Fig. 5. Charge distributions in the projected *xz* plane (y = 0) of the 3D simulation domain at t = 0, 0.2 and 2 ps after the deposition of 10 × 4000 electrons along a 1-µm length track located at 1.5 µm from the contact. Same simulation parameters as used and reported in the caption of Fig. 4.

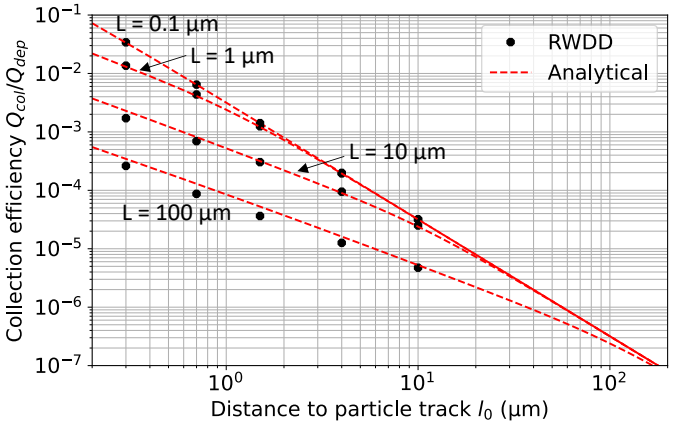

Fig. 6. Collection efficiency of a collecting contact analytically predicted by (15) and numerically computed using a Monte Carlo RWDD simulation code for a particle track of length L located at distance l_0 from the collecting contact (see configuration in Fig. 2).

Fig. 5 shows an example of RWDD simulation reproducing the irradiation configuration of Fig. 2 for a 1 µm length track located at 1.5 µm from the contact. The track is fragmented in 10 parts, each part or segment $d\ell = 0.1$ µm carries $\delta n_0 = 4{,}000$ electrons. The collecting efficiency was evaluated at the end of the simulation by calculating the ratio of the number of collected electrons by the total number of deposited electrons.

Fig. 6 shows the comparison of these numerical data with analytical predictions made using (15). A very nice agreement is observed on the full distance range, especially for short particle tracks, up to 10 µm. For the very long track corresponding to L = 100 µm, a slight difference is visible for $l_0 < 4$ µm, presumably due to intrinsic stochastics error in RWDD simulation when the distance between track segments and the collecting contact become important and the number of particles involved in the simulation is limited (due to computer memory).

III. Soft Error Rate Modeling in the Diffusion-Collection Approximation

From the above equations and in the framework of the diffusion-collection model, we can now derivate an analytical expression for the soft error rate of a circuit element for which a sensitive node is represented by the simple geometry shown in Figs. 2 and 7. Considering a given critical charge value Q_{crit} for the circuit element being modeled, (13) immediately shows that there is a critical distance from the sensitive node below which any ion impact will lead to an upset

$$l_{crit} = L \times \left[sinh\left(\frac{Q_{crit}}{Q_0} \right) \right]^{-1} \qquad (17)$$

As illustrated in Fig. 7, l_{crit} defines a disk centered in the sensitive node P; any ion impact in the disk will result in $Q_{col} \geq Q_{crit}$ and thus in an upset.

The number of upsets per unit time, i.e. the soft error rate, is thus simply equal to the product of the disk surface πl_{crit}^2 by the particle flux F, that gives

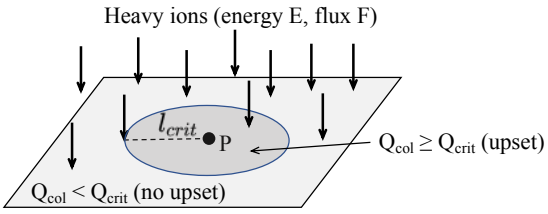

Fig. 7. Sensitive area defined by the disk of radius l_{crit}.

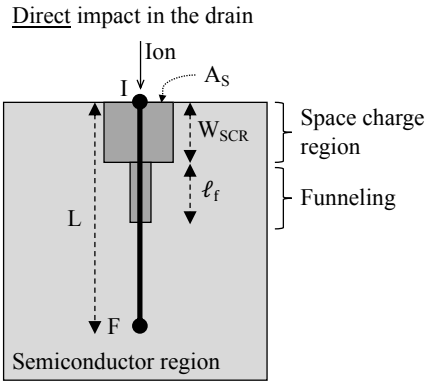

Fig. 8. Schematic for a direct particle impact in the drain.

$$SER = \pi l_{crit}^2 F = \pi L^2 F \times \left[sinh\left(\frac{Q_{crit}}{Q_0} \right) \right]^{-2} \qquad (18)$$

The surface πl_{crit}^2 corresponds to the heavy ion cross-section of the modeled circuit node in the approximation of the diffusion-collection approach [5]. Equation (18) is also valid in the framework of the above approximations, whatever the values of L, l_0 and Q_{crit}. It represents a general expression for the SER of a circuit element subjected to a perpendicular heavy ion beam and characterized by a critical charge Q_{crit} and a sensitive node with a sufficiently "small" surface to avoid charge integration over the drain area and to use the approximation of (4).

From (18), it is now easy to derive an expression very close to the empirical expression proposed by Hazucha and Svensson [1]. Remembering that $sinh(x) = (e^x - e^{-x})/2$, in the particular case where $Q_{crit} >> Q_0$, we obtain the following approximation for the critical length and for the SER

$$l_{crit}(Q_{crit} \gg Q_0) = 2L \times exp\left(-\frac{Q_{crit}}{Q_0} \right) \qquad (19)$$

$$SER(Q_{crit} \gg Q_0) = 4\pi L^2 F \times exp\left(-\frac{Q_{crit}}{Q_0/2} \right) \qquad (20)$$

The collection slope Q_S, introduced in (1), is found to have the following expression

$$Q_S = \frac{Q_0}{2} = \frac{q A_S v_{col} N}{8\pi D^* L} \qquad (21)$$

Equation (18) is related to the SER induced by the diffusion of deposited charge outside the sensitive drain, due to the "point surface" approximation made in (4). For direct impacts, another expression of the SER should be considered, as illustrated in Fig. 8 and detailed in the following. In this case, the collected

charge has two components:

1) a charge Q_1 directly deposited and collected in the space charge region augmented by a possible funneling mechanism (if $L > W_{SCR}$);
2) a charge Q_2 deposited in the substrate below the junction and collected via the diffusion-collection process if $L > (W_{SCR} + \ell_f)$.

From notations of Fig. 2 and considering $L > (W_{SCR} + \ell_f)$, we can write

$$Q_1 = \frac{qN}{L} \times (W_{SCR} + \ell_f) \tag{22}$$

$$Q_2 = \frac{qA_S v_{col} N}{4\pi D^* L} \int_{W_{SCR}+\ell_f}^{L} \frac{d\ell}{\ell} = Q_0 \times ln\left(\frac{L}{W_{SCR} + \ell_f}\right) \tag{23}$$

where the length of collection ℓ_f related to funneling is given by [21]

$$\ell_f = \left(1 + \frac{\mu_n}{\mu_p}\right) W_{SCR} \tag{24}$$

If $(L < W_{SCR} + \ell_f)$, $Q_2 = 0$ and $Q_1 = qN$.

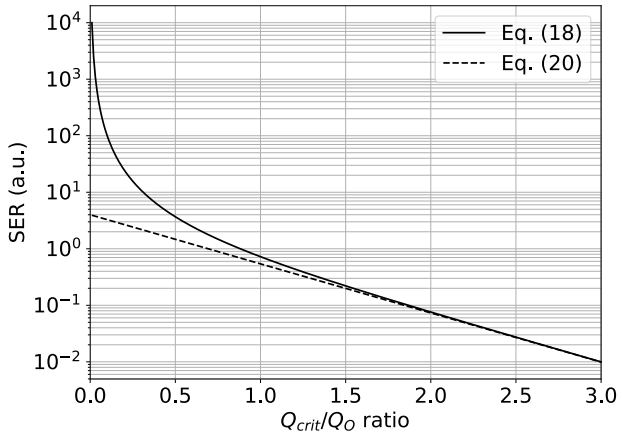

Fig. 9. Comparison of values given by expressions (18) and (20) as a function of the Q_{crit}/Q_0 ratio. To facilitate comparison, the quantity $\pi L^2 F$ was fixed equal to 1 in the two expressions.

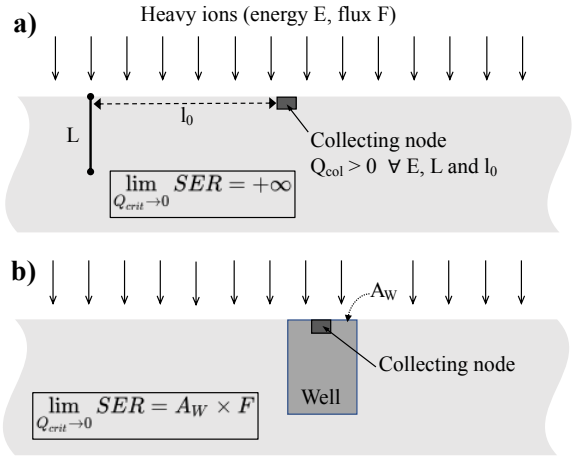

Fig. 10. Schematics illustrating the difference in SER limit when Q_{crit} tends towards zero (without carrier recombination): a) collecting node integrated in an "infinite" semiconductor domain and b) collecting node integrated in a finite dimension well. A_W corresponds to the well top surface.

From the above equations, the SER component due to the sole contribution of direct impacts in the drain area is thus expressed as

$$SER^{DI} = \begin{cases} 0 & if\ (Q_1 + Q_2) < Q_{crit} \\ A_S F & if\ (Q_1 + Q_2) \geqslant Q_{crit} \end{cases} \tag{25}$$

Eq. (25) implicitly underlies the notion of critical *LET* for the incident ions able to trig an upset. Unfortunately, the equation $Q_1 + Q_2 = Q_{crit}$ has no analytical solution for the ratio L/N and must be numerically solved.

IV. Discussion

A. About the Hazucha and Svensson's expression

Equation (20) is almost the same as the empirical expression proposed by Hazucha and Svensson. In particular, the development of our model from the basic equations of the collection-diffusion approach highlights the physical origin of the exponential dependence of the SER with critical charge: the charge transport via a pure diffusion process.

A similar result was previously obtained by Edmonds in the appendix of Ref. [5] for a sensitive node array separated by reflective surfaces and subjected to heavy ions (perpendicularly incident to the array surface): the node cross-section X for collected charge to exceed a certain value Q was expressed under the form X = B exp[-Q/(aAL)] where A and B are two geometric constants (not expressed), L is the ion LET and a is a conversion unit constant for silicon. In the present work, this exponential term in the expression of the SER is found to derive from the hyperbolic sine function for large values of the argument: it corresponds to values of Q_{crit} larger than Q_0. Fig. 9 directly compares normalized SER values obtained from (18) and (20). This plot shows that the exponential approximation is valid as soon as Q_{crit}/Q_0 is typically larger than 1.5. For smaller ratio values, the SER deviates from the exponential law and it becomes necessary to consider the hyperbolic sine.

A notable difference between (1) and (20) comes from the dependency with the drain area. In the Hazucha and Svensson's formula, the SER is directly proportional to A_S (which is clearly intuitive, notably for direct particle impacts on the drain area) whereas in (18) (and also in (20)), this dependency is only included in the term Q_0. At this level, the "point surface" approximation made in (4) – which implies that (20) only consider impacts outside the drain surface – may explain this difference in the surface dependence of the SER.

On one hand, it is quite remarkable that Hazucha and Svensson formulated (1) on the sole basis of experimental data obtained from atmospheric neutron irradiation. Several of their remarks written in [1] take on their full meaning in the light of these analytical developments. In particular, from (1) commented in [1]: "*κ should not depend on* V_{DD} *or doping profiles. […] Collection slope* Q_S *depends strongly on doping and* V_{DD}". These remarks are fully valid for (20): the prefactor term $4\pi L^2$ does not depend on V_{DD} or doping levels (profiles). Collection slope Q_S, given by (21), depends on doping and V_{DD}, as explained in III.B. It must be also noted that both the

prefactor and exponential terms depend, in our developments, on the type and characteristics of radiation.

On the other hand, another remark of Hazucha and Svensson about (1) is the following [1]: "*Extrapolations to $Q_{crit} = 0$ gives* SER = $\kappa \times A_S \times F$. *Cross section at this point is determined by the rate at which the secondary particles intercept the drain, rather than by the amount of collected charge".* If this remark is *a priori* attractive, it is because, in the compact form of (1), this expression links with a continuous and unified expression (owing to the property of the exponential function which equals 1 in 0), a formulation of the SER for both direct impacts in the drain and indirect impacts by diffusion-collection. But we believe that this way of doing things is quite inconsistent on the physical point-of-view. Indeed, a sensitive node of a circuit whose critical charge tends towards zero becomes sensitive to *all* the particles which deposit a charge near this node. In the hypothetical case where a sensitive node would be integrated alone within a semiconductor domain extending to infinity and subjected to radiation, as illustrated in Fig. 10a, the soft error rate resulting from the diffusion-collection of the deposited charges would be infinite (neglecting carrier recombination), as predicted by (18) for Q_{crit} which tends to 0 (see also Fig. 9). More realistically, the SER value should reach an upper (large) limit value (which has nothing to do, and which is much higher than $A_S \times F$) due to carrier recombination which screens minority carriers deposit beyond a certain distance.

But this view is only theoretical since a sensitive node in a CMOS circuit is not isolated but always integrated in a semiconductor well (p-well for NMOS, n-well for PMOS) which has lateral finite dimensions and/or limited depth extension (see Fig. 10b). This means that the quantity of deposited charges in the relevant well is a finite quantity. In this case, if the critical charge of the sensitive node tends towards zero, this implies that all particles impacting the well will upset the sensitive node because, from (13), whatever the values of N, L and l_0 for any trace of the particle in the well, the collected charge by the sensitive node will never be zero, therefore even very small but always higher than Q_{crit}. This reasoning demonstrates that the SER of a nearly zero critical charge circuit is not infinite but tends towards an upper limit which only depends on the geometry of the circuit and the characteristics of the particle flux. In the simplified view illustrated in Fig. 10b, this SER limit value is $A_W \times F$, where A_W is the well top surface. In (1), this limit is expressed by the quantity $\kappa \times A_S \times F$, the parameter κ contributing to fit the expression to the true surface to consider, which is not equal to A_S but rather to a value considering the local environment (well geometry) of the sensitive node. In (18) or (20), the dependency of the SER due to collection-diffusion with the drain surface is included in the term Q_0, not in the prefactor term of these equations. For direct impacts, the quantity to consider is well $A_S \times F$, as used in (25).

B. Supply voltage dependence

The SER model of (18) presents a dependence with the supply voltage V_{DD} via both v_{col} and Q_{crit} terms.

Concerning the collection velocity, v_{col} can be derived from the average value of the drift velocity in the SCR region of the drain junction [13]

$$v_{col} \approx \mu_n \frac{F_{max}}{2} = \mu_n \frac{(V_{bi} + V_R)}{W_{SCR}} \tag{26}$$

where F_{max} is the maximum value of the electric field, μ_n is the electron mobility, V_{bi} is the internal barrier potential, $V_R = V_{DD}$ is the reverse bias applied to the N^+ contact and W_{SCR} is the width of the space charge region [22]

$$V_{bi} = \frac{kT}{q} ln\left(\frac{N_A N_D}{n_i^2}\right) \tag{27}$$

$$W_{SCR} = \sqrt{\frac{2\epsilon_{SC}(V_{bi} + V_R)}{qN_A}} \tag{28}$$

with N_A and N_D are the doping levels for p-type and n-type regions respectively, n_i is the intrinsic carrier concentration of the semiconductor material, and ε_{SC} is the semiconductor dielectric constant.

Inserting (26) in (14) using (27) and (28) gives

$$Q_0 = \frac{q\mu_n A_S N}{4\,\pi D^* L}\sqrt{\frac{qN_A(V_{bi} + V_R)}{2\epsilon_{SC}}} \tag{29}$$

For the critical charge, in the case of an SRAM cell, Q_{crit} can be modeled as a sum of capacitance and conduction components of the impacted node [2]

$$Q_{crit} = C_N V_{DD} + I_{DP} t_F \tag{30}$$

where C_N is the equivalent capacitance of the struck node, V_{DD} is the supply voltage, I_{DP} is the maximum current of the on-state pMOS transistor and t_F is the cell flipping time.

At this level, different refinements can be introduced to model the transistor on-state current and the cell flipping time or to use a more accurate integral expression of Q_{crit} considering the exact value of the static tripping point of the SRAM cell [23-27]. Analysis of modeling and simulation results [28] suggest that critical charge variations can be linearized around the value obtained for the nominal core voltage. A first-order approximation can be written under the form

$$Q_{crit}(V_{DD}) \approx Q_{crit,nom} + \alpha(V_{DD} - V_{DD,nom}) \tag{31}$$

where $Q_{crit,nom}$ is the critical charge at nominal core voltage $V_{DD,nom}$ and α is a voltage variation coefficient which can be extracted from SPICE or TCAD simulations.

Equations (18), (29) and (31) are the core equations of the SER(V_{DD}) model. Fig. 11 shows comparison of experimental SER data with model predictions. Data were obtained from a CMOS bulk 65 nm single-port SRAM test vehicle subjected to accelerated alpha irradiation using a ^{241}Am source [29-30]. The core voltage for this technology is $V_{DD,nom}$ = 1.2 V. Due to the very short distance between the source emitting surface and the circuit surface (< 1 mm) and although the source is isotropic, mostly alpha particles inducing upsets can be assumed to arrive perpendicularly to the surface. SER was measured within a voltage range of ±20% around $V_{DD,nom}$. In Fig. 11, data is

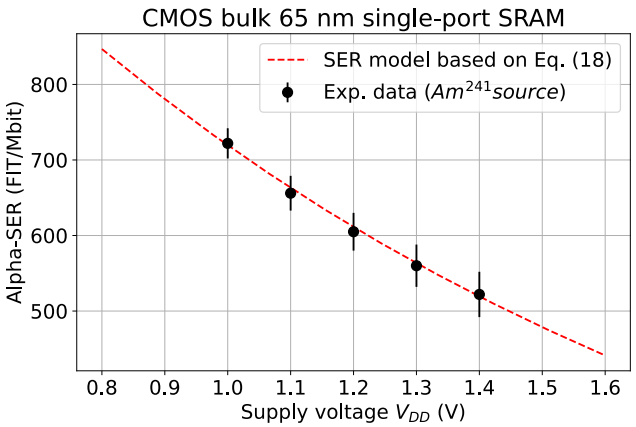

Fig. 11. Alpha-SER dependence with the supply voltage in a CMOS bulk 65nm single-port SRAM. Experimental values have been measured using a ^{241}Am source (5.46 MeV alpha particles). The dashed line corresponds to SER values calculated from (18), (29) and (31) and converted in FIT/Mbit with geometrical and technological parameters reported in [29-30]. For industrial confidentiality reason, all numerical results in this figure have been normalized by a common arbitrary scaling factor, set lower than 3. The real order of magnitude for the reported data is thus not significantly altered.

compared to SER values calculated from (18), (29) and (31) (expressed in FIT/Mbit) with geometrical, technological and circuit parameters reported in [29-30]. The model (dashed line) fits the experimental data very well and, in particular, is able to reproduce the nonlinear behavior of SER with V_{DD} in this voltage range. It should however be noted that, to optimize the model curve with respect to experimental data, the ambipolar coefficient and the voltage variation coefficient α have been fine-tuned. In this way, the SER model curve of Fig. 11 corresponds to Q_{crit} = 1.8 fC [31] and α = 1.15 fC.V^{-1}. This last value matches circuit simulation for bulk 65 nm with an extracted value around 1 fC.V^{-1}.

C. *Model characterization and exploration*

The developed analytical SER model needs the knowledge of a certain number of physical, geometrical and electrical parameter values to be properly used. These parameters include:

- the critical value of the node element Q_{crit} and possibly its dependence with V_{DD} obtained by circuit simulation;
- the drain area of the sensitive transistor As;
- the characteristics of the incoming ionizing radiation that is required to evaluate the particle range L and the ratio N/L of deposited pairs per unit length;
- the ambipolar diffusion coefficient D^*, that requires the knowledge of both electron and hole mobilities μ_n and μ_p in the substrate of transistor well region;
- ideally the technological structure of the drain to evaluate the collection velocity v_{col} from the basic equations of the P-N junction (26-28) or by TCAD simulation [15].

However, in case of one or both of these last parameters (i.e., D^* and v_{col}) may be hard to access without accurate fabricating information or difficult to evaluate (v_{col} is very sensitive to the drain architecture in terms of doping and electric field distributions), it can be envisaged to consider them as fitting parameter(s) of the model, since the others are supposed to be known. This approach is largely used in the domain [7-15].

To complete results presented in IV.B, we used our model to provide quantitative trends for different technological nodes (bulk 45, 32, 22 and 16 nm) concerning their voltage dependency. Results are shown in Fig. 12. For these calculations, Q_{crit} versus V_{DD} values were taken from Fig. 5a in [32], the other values were estimated from the International Technology Roadmap for Semiconductors [33] and by scaling some parameters of the bulk 65nm SRAM. As discussed in previous works [34-36], the observed SER improvement induced by the scaling of the planar processes is found to be roughly a combination of the bit-cell area and V_{DD} reductions, in good agreement with other published data (see for example the overall scaling trend for memories in [36]).

D. *Planar versus FinFET architectures*

The geometrical configuration shown in Figs. 2 and 8 typically corresponds to the case of planar transistors. Another interesting configuration corresponds to that of the FinFET architecture. The 3D topology of the FinFET strongly modifies the way that radiation-induced charges are collected with respect to the case of planar FET. This aspect is illustrated in Fig. 13 and has been addressed in recent works [37-42]. As shown in Fig. 13, the situation changes for indirect impacts whereas for direct impacts (i.e., for particle strike in the fin), the situation is identical to that described in Fig. 8 and (24) remains valid.

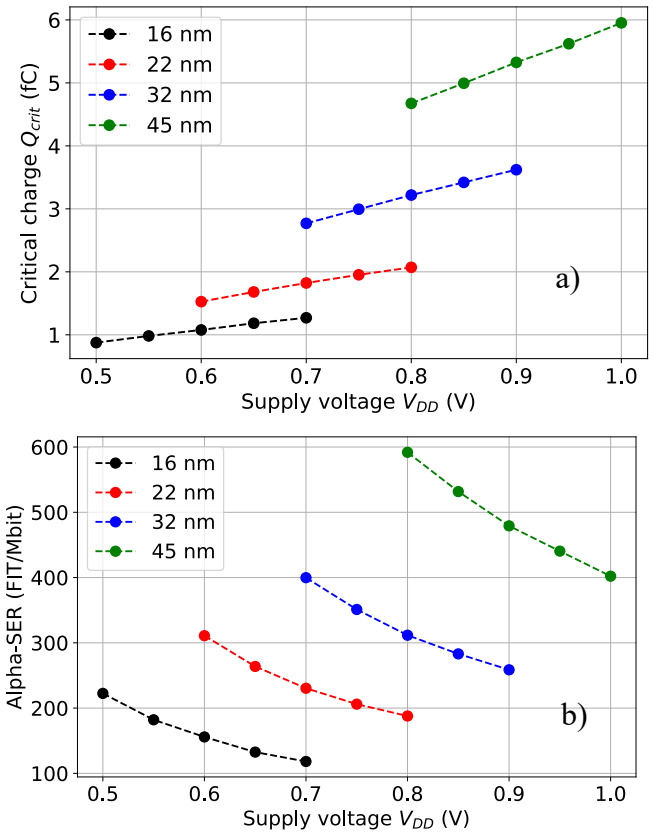

Fig. 12. Critical charge (a) and alpha-SER (b) versus V_{DD} estimated for generic SRAMs designed in CMOS bulk 45, 32, 22 and 16 nm. Q_{crit} versus V_{DD} values were taken from Fig. 5a in [32]. SER values are calculated from (18), (29) and (31) for an alpha emissivity of 10^{-3} α/cm^2/h. Other simulation parameters are: D^* = 8.6 cm^2/s, As = 0.0165 µm^2 for the 45 nm node, alpha-particles of 5.46 MeV with L = 28µm.

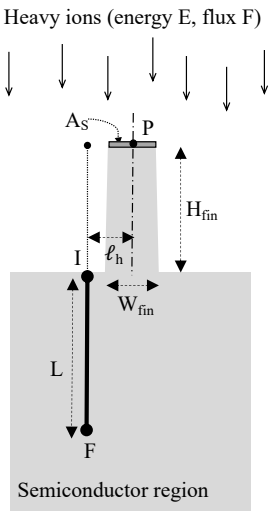

Fig. 13. Charge collection process in a FinFeT device for an indirect impact at the base of the fin (inspired from Monga et al. [37] for the ion track and device configuration).

Although the aim of this paper is not to develop a complete model for the FinFET architecture, it seems interesting to try to express the SER for a geometry that approximates the topology of these non-planar structures from the previous analytical developments. In the case of an indirect impact, illustrated in Fig. 13 and inspired from the work of Monga et al. [37], we can see that the charge integration performed in (10) must be modified to roughly take into account this new geometry

$$Q_{col} \approx Q_0 \int_0^1 \frac{(L+H_{fin})d\lambda}{\sqrt{\ell_h^2+\lambda^2(L+H_{fin})^2}} - Q_0 \int_0^1 \frac{H_{fin}d\lambda}{\sqrt{\ell_h^2+\lambda^2 H_{fin}^2}} \quad (32)$$

Equation (32) is therefore an approximation of the collected charge in FinFET-like architecture because this evaluation treats charge collection at the substrate region (from the bottom of the fin to L) as the same as the planar one. Indeed, for example, the shortest collecting path for charge deposited near H_{fin} depth is prohibited by the shallow trench isolation (STI) layer, so such asymmetry should theoretically influence the collecting efficiency and thus the collected charge value. In the framework of this important simplification and from (32), we obtain

$$Q_{col} = Q_0 \left[arsinh\left(\frac{L+H_{fin}}{\ell_h}\right) - arsinh\left(\frac{H_{fin}}{\ell_h}\right)\right] \quad (33)$$

Equation (33) is identical to (13) when $H_{fin} = 0$ and $\ell_h = l_0$. The first term represents the contribution to the collected charge of a track of total length $L+H_{fin}$ from which the contribution of the virtual track of length H_{fin} is subtracted.

The second term of (33) admits a maximum value when $\ell_h = W_{fin}/2$, the minimum distance for an indirect impact. Indeed, it was shown in [41] that ion strikes in the substrate region of a FinFET do not result in enough charge collected to produce measurable transients. This was confirmed by 3D TCAD simulation: the collection efficiency is found to drop off to a few percents or less in the substrate [41]. From this result and in addition to direct ion impacts in the fin structure, we can reasonably speculate that only indirect particle strikes in the close vicinity of the fin base should contribute to the SER. For ion track lengths above a few tens of nanometers that is generally the case, $L+H_{fin} \approx L$. We deduce from the following approximation a simple expression for l_{crit} in the case of indirect ion impacts in a FinFET architecture

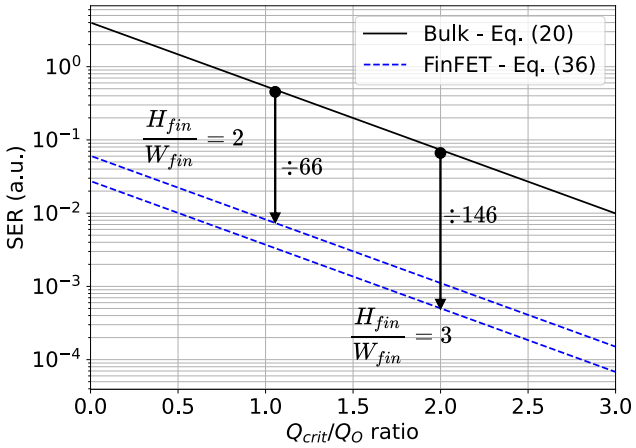

Fig. 14. Reduction of the SER for FinFET with respect to planar structures as predicted by (20) and (36).

$$l_{crit} = L \times \left[sinh\left(\frac{Q_{crit}}{Q_0} + \gamma\right)\right]^{-1} \quad (34)$$

with

$$\gamma = arsinh\left(\frac{2H_{fin}}{W_{fin}}\right) \quad (35)$$

that gives

$$SER = \pi L^2 F \times \left[sinh\left(\frac{Q_{crit}}{Q_0} + \gamma\right)\right]^{-2} \quad (36)$$

The geometrical factor γ characterizes the fin architecture. Its value increases with the height of the fin and decreases with its width. γ reduces to 0 for planar architectures. This dimensionless factor is added to the ratio Q_{crit}/Q_0 in the argument of the *sinh* term, which has the effect of reducing the value of the SER (i.e., equivalent to an increase of Q_{crit}). The FinFET architecture therefore appears to be intrinsically more immune to radiation because charge collection is reduced for transistor geometry reasons, which is precisely expressed by the gamma factor in this equation. The more the thin has an elongated architecture, the smaller the collection of charges and therefore the better its resistance to radiation.

To conclude, when $Q_{crit}/Q_0 + \gamma > 1.5$ (which is always the case if $H_{fin} > W_{fin}$), the hyperbolic sine can be replaced by a simple exponential, and we have

$$SER = 4\pi L^2 F \times exp\left[-\left(\frac{Q_{crit}}{Q_0/2} + 2\gamma\right)\right] \quad (37)$$

Incidentally, (37) shows that the exponential dependence of the SER with Q_{crit} is conserved in FinFET architectures, which was empirically observed and accepted up to now.

Fig. 14 illustrates the reduction of the SER for FinFET with respect to planar structures as predicted by (20) and (36). Due to the simplicity of the above model, the reduction factors reported in Fig. 14 for two fin elongations ($H_{fin}/W_{fin} = 2$ and 3) should be considered with caution and considered more qualitatively than quantitatively. Further developments and validation of the model remain necessary at this stage.

CONCLUSION

From the basic equations of the diffusion-collection model, we derived in this study an analytical soft error rate model dedicated to CMOS circuit elements for which the critical charge concept can be applied. We found a simple expression for the SER involving the hyperbolic sine of the critical charge. For a certain condition on the value of the critical charge, given by the model, this expression can be simplified. It shows in this case an exponential dependence of the SER with Q_{crit}, under the same form as empirically proposed by Hazucha and Svensson in [1]. Coming after the pioneering works of Edmonds [4-5], the present contribution also establishes from physics-based equations the origin of the exponential term in this expression: the charge transport via a pure diffusion process. Our analytical formulation also links the SER with physical and technological parameters, notably carrier diffusion coefficient, drain structure, ion characteristics and circuit supply voltage. For this last parameter, we pushed the development of our model to obtain a set of analytical expressions able to numerically estimate SER variations with supply voltage. This point was validated with data obtained from alpha-particle accelerated irradiation performed on a CMOS bulk 65 nm single port SRAM test vehicle. We also provide quantitative trends for different technological nodes (bulk 45, 32, 22 and 16 nm) concerning their voltage dependency. Finally, we proposed a derivation of our model for FinFET architectures that, more qualitatively than accurately at this preliminary level of development, evidences the intrinsic reduction of the SER in FinFET due to the 3D geometry. This reduction factor is found to be linked to the characteristics (height and width) of the fin. Further developments are calling to consolidate and characterize a complete model from the proposed approach.

ACKNOWLEDGMENT

The authors would like to thank their colleagues Dr. P. Roche, Dr. G. Gasiot and Dr. V. Malherbe from STMicroelectronics (Crolles, France) for stimulating discussions and for their help in validating the model with experimental data.

REFERENCES

[1] P. Hazucha and C. Svensson, “Impact of CMOS Technology Scaling on the Atmospheric Neutron Soft Error Rate,” *IEEE Trans. Nucl. Sci.,* vol. 47, no. 6, pp. 2586-2594, Dec. 2000.

[2] J.L. Autran, D. Munteanu. *Soft errors: from particles to circuits*. Boca Raton: CRC Press, 2015.

[3] S. Kirkpatrick, “Modeling diffusion and collection of charge from ionizing radiation in silicon devices,” *IEEE Trans. Electron Devices*, vol. 26, no. 11, pp. 1742-1753, Nov. 1979.

[4] L. D. Edmonds, "Charged collected by diffusion from an ion track under mixed boundary conditions," *IEEE Trans. Nucl. Sci.,* vol. 38, no. 2, pp. 834-837, April 1991.

[5] L. D. Edmonds, "SEU cross sections derived from a diffusion analysis," *IEEE Trans. Nucl. Sci.,* vol. 43, no. 6, pp. 3207-3217, Dec. 1996.

[6] G. C. Messenger, "Collection of Charge on Junction Nodes from Ion Tracks," *IEEE Trans. Nucl. Sci.*, vol. 29, no. 6, pp. 2024-2031, Dec. 1982.

[7] J.M. Palau, G. Hubert, K. Coulie, B. Sagnes, M.C. Calvet, S. Fourtine, “Device simulation study of the SEU sensitivity of SRAMs to internal ion tracks generated by nuclear reactions,” *IEEE Trans. Nucl. Sci.*, Vol. 48, no. 2, pp. 225–231, April 2001.

[8] G. Hubert, “Elaboration d'une méthode de prédiction du taux d'aléas logiques induits dans les mémoires SRAM par les neutrons atmosphériques,” Ph.D. Thesis, Université Montpellier II, 2002.

[9] T. Merelle et al., “Criterion for SEU occurrence in SRAM deduced from circuit and device Simulations in case of neutron-induced SER,” *IEEE Trans. Nucl. Sci.*, vol. 52, no. 4, pp. 1148-1155, Aug. 2005.

[10] D. Lambert, “Analyse par simulation Monte Carlo de la sensibilité aux aléas logiques des mémoires SRAM soumises à un environnement protonique spatial ou neutronique terrestre,” Ph.D. Thesis, Université Montpellier II, 2006.

[11] F. Wrobel, G. Hubert and P. Iacconi, "A Semi-empirical Approach for Heavy Ion SEU Cross Section Calculations," *IEEE Trans. Nucl. Sci.*, vol. 53, no. 6, pp. 3271-3276, Dec. 2006.

[12] V. Correas, “Prédiction de la section efficace des aléas logiques (SEU) et du taux d’aléas multiples (MCU) de technologies CMOS deca-nanométriques sous irradiation aux ions lourd ”, Ph.D. Thesis, Université Montpellier II, 2008.

[13] L. Artola, G. Hubert, S. Duzellier and F. Bezerra, “Collected Charge Analysis for a New Transient Model by TCAD Simulation in 90 nm Technology,” *IEEE Trans. Nucl. Sci.*, vol. 57, no. 4, pp. 1869-1875, Aug. 2010.

[14] L. Artola et al., "SEU Prediction From SET Modeling Using Multi-Node Collection in Bulk Transistors and SRAMs Down to the 65 nm Technology Node," *IEEE Trans. Nucl. Sci.*, vol. 58, no. 3, pp. 1338-1346, June 2011.

[15] S. Uznanski. *Single Event Upsets in Sub-65nm CMOS technologies: Monte-Carlo simulations and contribution to understanding of physical mechanisms.* London: LAP Lambert Academic Publishing, Dec. 2011.

[16] J.L. Autran, S. Semikh, D. Munteanu, S. Serre, G. Gasiot, P. Roche, “Soft-Error Rate of Advanced SRAM Memories: Modeling and Monte Carlo Simulation”, in *Numerical Simulation - From Theory to Industry*, Edited by M. Andriychuk. Vienna: IntechOpen, Chapter 15, 2012.

[17] R.B. Paris, “Incomplete Gamma and Related Functions”, in *NIST Handbook of Mathematical Functions*, Edited by Frank W.J. Olver, Daniel W. Lozier, Ronald F. Boisvert and Charles W. Clark. Cambridge: Cambridge University Press, Chapter 8, 2010.

[18] M. Glorieux, J. L. Autran, D. Munteanu, S. Clerc, G. Gasiot and P. Roche, "Random-Walk Drift-Diffusion Charge-Collection Model For Reverse-Biased Junctions Embedded in Circuits," *IEEE Trans. Nucl. Sci.*, vol. 61, no. 6, pp. 3527-3534, Dec. 2014.

[19] J.L. Autran, M. Glorieux, D. Munteanu, S. Clerc, G. Gasiot, P. Roche, “Particle Monte Carlo modeling of single-event transient current and charge collection in integrated circuits,” *Microelectronics Reliability*, vol. 54, no. 9-10, pp. 2278-2283, Sept.-Oct.2014.

[20] J.L. Autran, D. Munteanu, S. Moindjie, T. Saad Saoud, V. Malherbe, G. Gasiot, S. Clerc, P. Roche, “Charge Collection Physical Modeling for Soft Error Rate Computational Simulation in Digital Circuits," in *Modeling and Simulation in Engineering Sciences*, Edited by N. Sher Akbar and O. Anwar Beg. Vienna: IntechOpen, Chapter 6, 2016.

[21] C. Hu, “Alpha-particle-induced field and enhanced collection of carriers,” *IEEE Electron Dev. Lett.*, vol. 3, no. 2, pp. 31-34, Feb. 1982.

[22] S. M. Sze, *Physics of Semiconductor Devices, 2nd ed.* New York: Wiley, 1981.

[23] B. Zhang, A. Arapostathis, S. Nassif, and M. Orshansky, "Analytical modeling of SRAM dynamic stability," *Proceedings of the IEEE/ACM International Conference on Computer-Aided Design*, pp. 315-322, 2006.

[24] S.M. Jahinuzzaman, M. Sharifkhani, and M. Sachdev, "An Analytical Model for Soft Error Critical Charge of Nanometric SRAMs", *IEEE Trans. Very Large Scale Integr. (VLSI) Syst.,* vol. 17, no. 9, pp. 1187-1195, Sept. 2009.

[25] H. Mostafa, M. Anis and M. Elmasry, "A Design-Oriented Soft Error Rate Variation Model Accounting for Both Die-to-Die and Within-Die Variations in Submicrometer CMOS SRAM Cells," *IEEE Transactions on Circuits and Systems I: Regular Papers*, vol. 57, no. 6, pp. 1298-1311, June 2010.

[26] H. Mostafa, M. Anis and M. Elmasry, "A Bias-Dependent Model for the Impact of Process Variations on the SRAM Soft Error Immunity," *IEEE Transactions on Very Large Scale Integration (VLSI) Systems*, vol. 19, no. 11, pp. 2130-2134, Nov. 2011.

[27] G. Torrens, S. A. Bota, B. Alorda and J. Segura, "An Experimental Approach to Accurate Alpha-SER Modeling and Optimization Through Design Parameters in 6T SRAM Cells for Deep-Nanometer CMOS," *IEEE Transactions on Device and Materials Reliability*, vol. 14, no. 4, pp. 1013-1021, Dec. 2014.

[28] T. Heijmen, D. Giot and P. Roche, "Factors that impact the critical charge of memory elements," *12th IEEE International On-Line Testing Symposium (IOLTS'06)*, pp. 6-12, 2006.

[29] D. Giot, "Study by numerical simulation of the sensitivity of SRAM memories in 90 and 65 nm technologies to the terrestrial radiative environment", Ph.D. Thesis, Aix-Marseille University, 2010.

[30] J.L. Autran, P. Roche, S. Sauze, G. Gasiot, D. Munteanu, P. Loaiza, M. Zampaolo, and J. Borel "Altitude and Underground Real-Time SER Characterization of CMOS 65 nm SRAM," *IEEE Trans. Nucl. Sci.*, vol. 56, no. 4, pp. 2258-2266, Aug. 2009.

[31] S. Serre, S. Semikh, S. Uznanski, J.L. Autran, D. Munteanu, G. Gasiot, P. Roche, "Geant4 Analysis of n-Si Nuclear Reactions From Different Sources of Neutrons and Its Implication on Soft-Error Rate", *IEEE Trans. Nucl. Sci.*, vol. 59, no. 4, pp. 714-722, Aug. 2012.

[32] J. Henkel, N. Dutt (Eds.). *Dependable Embedded Systems.* Cham: Springer International Publishing, 2021.

[33] International Technology Roadmap for Semi-conductors [online]. Available (2023, Jan. 13): http://www.itrs2.net/itrs-reports.html

[34] P. Roche, J.L. Autran, G. Gasiot and D. Munteanu, "Technology downscaling worsening radiation effects in bulk: SOI to the rescue," 2013 IEEE International Electron Devices Meeting, Washington, DC, USA, pp. 31.1.1-31.1.4, 2013.

[35] G. Hubert, L. Artola, D. Regis, "Impact of scaling on the soft error sensitivity of bulk, FDSOI and FinFET technologies due to atmospheric radiation," *Integration*, vol. 50, pp. 39-47, June 2015.

[36] I. Chatterjee, "From MOSFETs to FinFETs - The Soft Error Scaling Trends," RADNEXT tribune, 2020 [online]. Available (2023, Jan. 13): https://radnext.web.cern.ch/blog/from-mosfets-to-finfets/

[37] U. Monga et al., "Charge-collection modeling for SER simulation in FinFETs," *International Conference on Simulation of Semiconductor Processes and Devices*, pp. 295-298, 2016.

[38] S. Lee et al., "Radiation-induced soft error rate analyses for 14 nm FinFET SRAM devices," *IEEE International Reliability Physics Symposium*, pp. 4B.1.1-4B.1.4, 2015.

[39] T. Uemura et al., "Investigation of alpha-induced single event transient (SET) in 10 nm FinFET logic circuit," *IEEE International Reliability Physics Symposium*, pp. P-SE.1-1-P-SE.1-4, 2018.

[40] T. Thery, G. Gasiot, V. Malherbe, J.L. Autran and P. Roche, "TIARA: Industrial Platform for Monte Carlo Single-Event Simulations in Planar Bulk, FD-SOI, and FinFET," *IEEE Trans. Nucl. Sci.*, vol. 68, no. 5, pp. 603-610, May 2021.

[41] S. Agarwal et al., "Measuring and Modeling Single Event Transients in 12-nm Inverters," *IEEE Trans. Nucl. Sci.*, vol. 69, no. 3, pp. 414-421, March 2022.

[42] B. Narasimham, V. Chaudhary, M. Smith, L. Tsau, D. Ball and B. Bhuva, "Scaling Trends in the Soft Error Rate of SRAMs from Planar to 5-nm FinFET," *IEEE International Reliability Physics Symposium*, Monterey, CA, USA, pp. 7C.3.1-7C.3.5, 2021.